machines

MDPI

Article

Theoretical Design and Experimental Validation of a Vibro-Impact Support for Vibration Suppression

Diego Francisco Ledezma-Ramírez [1,*], Emiliano Rustighi [2] and Pablo Ernesto Tapia González [1]

[1] Facultad de Ingenieria Mecánica y Eléctrica, Universidad Autónoma de Nuevo León, San Nicolás de los Garza 66455, Nuevo León, Mexico; pablo.tapiagz@uanl.edu.mx
[2] Department of Industrial Engineering, University of Trento, 38122 Trento, Italy
* Correspondence: diego.ledezmard@uanl.edu.mx

Abstract

To mitigate the high contact forces and noise inherent in traditional hard-impact dampers, this work evaluates the efficacy of a soft viscoelastic vibro-impact interface for passive vibration suppression. This study investigates the nonlinear dynamic behavior of a cantilever beam equipped with a soft vibro-impact interface, combining theoretical modeling and experimental validation to explore energy redistribution and damping enhancement mechanisms. The system is excited under both free and forced vibration conditions, and its response is characterized through tip displacement, acceleration, and impact force measurements. Numerical simulations based on an impact-contact model accurately predict the amplitude-dependent broadening and frequency shift observed in the experiments, demonstrating that the soft impacts introduce nonlinear stiffness and effective damping. The comparison between theoretical and experimental frequency responses confirms that energy is transferred from the primary mode to higher harmonics, leading to broadband vibration attenuation. These findings provide experimental evidence of the nonlinear energy transfer mechanisms previously predicted, including harmonic resonance stimulation and nonresonant energy exchange. The results demonstrate that soft-contact vibro-impact dampers can be effectively tuned to exploit nonlinear dynamics for enhanced passive vibration suppression, bridging the gap between theoretical predictions and practical implementations.

Keywords: impact damper; vibration suppression; impacts; nonlinear vibration; machine vibration

1. Introduction

The ongoing advancement of high-speed industrial machinery and precision manufacturing systems demands advanced vibration control strategies to maintain operational accuracy and structural longevity. Traditional linear isolation methods often prove insufficient when addressing broadband or transient excitations typical in complex machine assemblies. Recently, there has been an increased interest in the application of nonlinear passive, active, or adaptive control and isolation strategies for vibration, shock, and impacts [1]. An idea for vibration suppression is to transfer the energy resulting from a shock to a secondary system or to higher modes rather than isolating the vibration. There are several categories within this concept. These devices exploit the nonlinearity of impacts and other phenomena such as nonlinear stiffness and dry friction to transfer the energy and dissipate vibrations.

Academic Editor: Tamara Nestorović

Received: 15 January 2026
Revised: 5 February 2026
Accepted: 9 February 2026
Published: 10 February 2026

1.1. State of the Art in Vibro-Impact Damping

The systems which leverage the dissipative interactions between granular materials and structural components to enhance damping efficiency are called impact dampers [2]. Other systems demonstrate energy transfer between modes such as in vibro-impacting cantilever beams [3]. Particle dampers rely on the impact of one or several particles, which are usually in the form of rigid balls within a container [4]. Single-mass and multiple-mass impact dampers have been considered for their high performance in reducing structural vibrations through adequate optimization of their parameters [5,6]. Akbar et al. [7] also focused on the effect of hard and soft impacts. This study proposes lining Single-Particle Impact Dampers (SPIDs) with viscoelastic materials to address the high impact forces and noise associated with traditional hard-impact designs. Experimental results show that soft impact dampers (specifically using polyurethane foam) reduce impact forces by 96% and noise levels by 11.55 dB compared to steel-on-steel impacts, while maintaining a 40% reduction in vibration amplitude at resonance. Momentum exchange impact dampers (MEIDs) are based on the collision of two interfaces and are sometimes referred to as vibro-impact attachments. The concept that a momentum exchange impact damper transfers part of the momentum to a damper mass to reduce the shock vibration of the system was presented by Son et al. [8] focusing on the application of MEIDs in the reduction in floor impact noise and vibrations, demonstrating their potential to improve acoustic comfort in buildings. Karayannis et al. [9] presented this concept investigating their ability to passively absorb and dissipate significant portions of shock energy applied to primary systems, finding improved isolation in a wide frequency range. These devices have been extensively studied for their effectiveness in reducing structural vibrations through energy dissipation by impact. Further investigations explored the energy transfer mechanisms in multi-body MEID configurations, revealing complex interactions that enhance damping efficiency [10]. These devices work on the concept of targeted energy transfer (TET) which has been central to the development of vibro-impact non-linear energy sinks (VI-NESs). Weidemann et al. and Li et al. [11,12] explored the response of VI-NESs in nonlinear modal energy exchange, considering chains of oscillators and multiple degree-of-freedom systems. The authors found that when properly tuned, a VI-NES can extract energy from the primary structure due to the inelastic impacts and nonlinear stiffness characteristics. As these systems depend on parameters such as gravity, friction and non-linear stiffness, complex interactions can appear between these factors, so tuning is important to achieve broadband vibration suppression [13].

On the other hand, active or semiactive dampers, where interface properties can be tuned, have also been studied extensively [14–16]. Advancements in active damping control have led to the development of active MEIDs, where external actuators modulate the damping effect, optimizing energy dissipation [17]. In aerospace applications, hybrid MEIDs have been proposed for spacecraft landing gear systems, integrating impact damping with other control strategies to mitigate landing shocks [18]. Recent innovations in material science have expanded the capabilities of impact dampers. The use of liquid crystalline elastomers (LCEs) in impact damping applications has been explored, demonstrating enhanced energy absorption properties [19,20]. Similarly, the incorporation of magnetorheological elastomers (MREs) into variable stiffness impact dampers has enabled adaptive performance in response to dynamic loading conditions [21]. Rahmat et al. [22,23] developed a control model for an MREs-based damper and investigated its performance under transient loads, showing that MREs can modulate stiffness and damping characteristics in real time, allowing semiactive control of impact forces. MEIDs have also been applied in marine engineering, where pre-straining spring mechanisms have been introduced to optimize impact damping for boat shock vibration control [24]. Other recent

applications involve the use of hybrid automotive dampers, combining viscous damping and multiple-impact mechanisms, demonstrating improved damping in high-frequency regions and suggesting applications in suspension systems [25]. Ganci et al. [26] developed tapered impact dampers in roadside traffic signal structures, achieving effective vibration mitigation under wind-induced oscillations. Darmawan et al. [27] studied aerospace applications that propose a smart impact damper based on previews for the landing gear of unmanned aerial vehicles (UAVs), highlighting its effectiveness of shock attenuation through simulation and experimental validations.

1.2. Nonlinear Dynamics and Modeling Challenges

The modeling of impact dampers is an important and challenging task. Seminal work by Karayannis [9] considered piecewise nonlinear models to represent the dynamics of the system and understand the energy dissipation mechanisms through repeated impacts where the coefficient of restitution is a key parameter that can lead to stable or unstable responses as studied by Li and Du [28]. Gong et al. examined the multi-state dynamics and model similarity in vibro-impact systems, finding transitions between periodic, quasiperiodic, and chaotic behavior, which is important to understand the robustness of these devices under broadband or transient excitations [29]. The effects of the system parameters, i.e., mass, stiffness, and symmetry effects have been extensively studied by Lizunov et al. [30]. Optimal performance was found for low stiffness and high damping at the impact interface, as it promotes targeted energy transfer through a broader range of excitations, considering a Hertzian model for the contact interface. The mass ratio between the primary structure and damper is also important, as a higher mass ratio leads to better energy transfer but might cause wear due to the larger number of impacts [31]. In addition, when using a double-sided damper, i.e., having impacts at two ends, it can outperform single-sided designs. Furthermore, when considering a double-sided design, asymmetry can lead to enhanced energy localization and dissipation [32]. However, these comprehensive studies present only theoretical analysis with no experimental validation. Thus, practical implementation and validation through laboratory or real-life scenarios remains an important venue for further research.

Several studies have revealed a rich array of nonlinear phenomena in vibro-impacting cantilever (VIC) beams, such as the emergence of subharmonics and superharmonics, period-doubling routes to chaos, chattering, and aperiodic motions [33–37]. For instance, Bishop et al. [34] mapped various zones of periodic and multi-periodic behavior in the frequency response of impacting beams and proved the possibility of periodic and multi-periodic behavior during repetitive impacts on the vibro-impacting beam. Other researchers focused particularly on the bifurcation and the chaotic transitions [37,38]. Gandhi and Vyas [39] proved that VICs are nonlinear oscillators which show amplitude jumps and resonance frequency shifts akin to the behaviour observed in the Duffing oscillators. For these reasons VICs have been deemed highly suitable for numerous engineering applications, from vibration energy harvesting [40] to innovative damping solutions as in nonlinear energy sinks and tuned damping devices [41,42]. Despite this progress, the intricate dynamics arising from resonant and non-resonant energy interactions in VICs are still not fully understood, representing a significant area for future research given their broad application potential.

1.3. Scope and Contribution of This Study

The design of the damper proposed in this work comprises an impacting mass attached to a cantilever beam that is subjected to a sudden release, which then impacts against a silicone rubber support. A mathematical model is first considered to predict the response,

and then an experimental design is presented for different stiffness configurations to investigate the effect on the impact suppression and calibrate the theoretical model with the experimental results. The main scientific contribution of this work is that, unlike previous studies that focus primarily on theoretical models of vibro-impact systems, this work offers a combined theoretical–experimental investigation of a cantilever-based impact damper using a viscoelastic silicone rubber interface. The use of a soft impact interface is another important part of this contribution, as most of the studies available consider hard impacts. While the vast majority of research on impact dampers focuses on hard interfaces governed primarily by momentum exchange and instantaneous restitution [7], recent developments have shifted attention toward the benefits of soft, deformable boundaries. For example, Zhang et al. [43] recently demonstrated that the use of viscoelastic structural damping mechanisms can fundamentally alter energy dissipation, enabling broadband absorption that goes beyond simple resonance. This supports the premise of the current study, where the introduction of a silicone rubber interface is shown to exploit material nonlinearity for enhanced vibration suppression, distinct from the rigid collisions found in traditional designs. The proposed setup allows for further controlled variation of stiffness and captures nonlinear dynamic effects that are then validated experimentally, demonstrating an adequate correlation between theory and practice, thus addressing a key gap in the current literature and offering new insights for practical impact damper design and calibration. In addition, considering a cantilever beam in the model allows for more realistic boundary conditions similar to structural components found in different engineering disciplines. Although the interface is considered linear, using silicone rubber as the impacting surface could lead to further advantages due to material nonlinearity and viscoelastic effects. By integrating nonlinear vibro-impact interfaces, such as the viscoelastic support proposed in this study, machine designers can exploit Targeted Energy Transfer (TET) to protect sensitive mechanical components from dangerous vibrations. This approach shifts the focus from simple isolation to dynamic energy redistribution within the machine structure, offering a robust solution for a wide spectrum of industrial applications, ranging from robotic actuators to aerospace landing systems.

2. Numerical Modeling

2.1. Model Configuration

The mathematical model considers a cantilever beam whose free-end can impact an elastic support separated by a clearance d from the beam tip. The schematics of the model are presented in Figure 1. The system response is evaluated for free and forced vibration as illustrated in the following subsections. The elastic support is modeled by a spring of stiffness k_1 and a damper with damping coefficient c_1 and connected in parallel. The cantilever beam is modeled as a Euler–Bernoulli beam. A modal superposition approach is adopted and the beam response is approximated by the first N modes and the relationship between the vector of actual displacements of the beam $\mathbf{x}_b$ and the modal coordinates vector $\mathbf{y}$ is given by

$$\mathbf{x}_b(t) = \mathbf{B}\mathbf{y}(t), \tag{1}$$

where $\mathbf{B}$ is the modal matrix made of the mass-normalized mode shapes vectors $\boldsymbol{\phi}^{(n)}$ of the cantilever beam:

$$\mathbf{B} = \begin{bmatrix} \boldsymbol{\phi}^{(1)} & \boldsymbol{\phi}^{(2)} & \dots & \boldsymbol{\phi}^{(N)} \end{bmatrix}. \tag{2}$$

The modal coordinates vector $\mathbf{y}$ contains all the modal responses $y_n(t)$

$$\mathbf{y}(t) = \begin{Bmatrix} y_1(t) & y_2(t) & \dots & y_n(t) \end{Bmatrix}^{\mathrm{T}} \tag{3}$$

Each modal response is obtained by solving the modal equation of motion by numerical integration using a fourth-order Runge–Kutta method. The n-th modal equation of motion is given by

$$\ddot{y}_n(t) + 2\zeta_n\omega_n\dot{y}_n(t) + \omega_n^2 y_n(t) = q_n(t) \tag{4}$$

where ω_n is the n-th natural frequency of the cantilever beam and ζ_n is the n-th modal damping ratio. The aluminum beam is assumed to be lightly damped so a value of $\zeta_n = 0.01$ was added to approximate the structural damping of the beam. This value was later confirmed in an experimental modal analysis using the impact hammer method, where the modal damping was obtained by a simple peak picking and half power estimation. Modal damping has also been added to each modal equation of motion to model vibration dissipation in the beam. The modal force, $q_n(t)$, which is computed at each time step, expresses the contact force with the support is given by

$$\mathbf{q}(t) = \mathbf{B}^{\mathrm{T}}\mathbf{f}(t) \tag{5}$$

where $\mathbf{f}(t)$ is the vector of the N forces applied at the same degrees of freedom at which the displacement vector $\mathbf{x}_b(t)$ was evaluated. Only two components of the vector are different from zero, where the external harmonic force is applied ($f_e(t) = F\mathrm{e}^{\mathrm{i}\omega t}$) in correspondence of the displacement $x_{b,f}$ and where the beam can come to contact with the elastic support ($f_c(t)$) in correspondence of the displacement $x_{b,c}$.

$$\mathbf{f}(t) = \begin{Bmatrix} 0 & \dots & F\mathrm{e}^{\mathrm{i}\omega t} & \dots & 0 & \dots & f_c(t) & \dots & 0 \end{Bmatrix}^{\mathrm{T}} \tag{6}$$

The contact force f_c is computed at each time-step and it is null when the beam is not touching the elastic support, that is $x_{b,c} \geq -d$. The contact force is instead

$$f_c(t) = k_1 x_{b,c}(t) + c_1 \dot{x}_{b,c}(t) \tag{7}$$

when the end of the beam pushes against the elastic support, that is when $x_{b,c} < -d$.

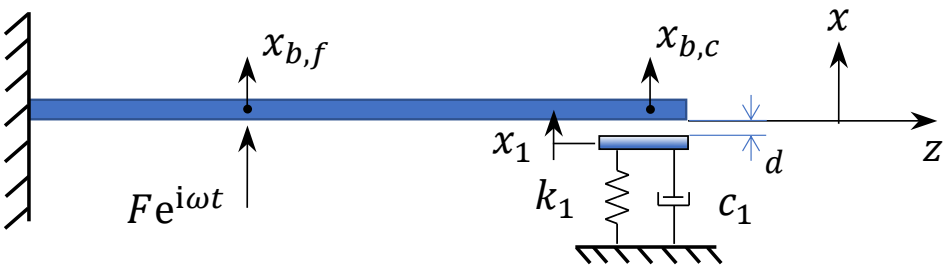

Figure 1. Model of a cantilever beam with a soft impact damper modeled as a spring damper in parallel located at its free end.

The free and forced response of the impact damper is analyzed in the following sections, considering a soft impacting interface. A slender aluminum beam is considered and approximated using Euler–Bernoulli beam theory. For the free response estimation, a prescribed static displacement is applied to the tip of the beam as an initial condition, so the motion starts when it is released. Different values of the initial displacement are considered. For forced vibrations, a sinusoidal input force is applied at a point in the beam. The parameters used in the modeling as well as further experimental validation are presented in Table 1. The natural frequencies were theoretically estimated using Euler–Bernoulli theory for slender beams and later confirmed by experimental modal analysis, while the input force was given by increasing the gain in the power amplifier in steps for each measurement. The response is obtained for different values of the frequency

and amplitude of the input signal. For both free and forced vibrations, tip displacement and acceleration, as well as contact force, are estimated through the simulations.

Table 1. Geometrical and experimental parameters of the vibro-impacting beam.

Parameter	Symbol	Value
Geometrical and material properties		
Beam length	L	0.40 m
Beam width	b	38 mm
Beam thickness	h	3 mm
Material	–	Aluminum
Impact gap	d	4 mm
Force application point	$x_{b,f}$	70 mm from fixed end
First five natural frequencies	f_n	15.4, 96.6, 270.6, 530.3, 876.6 Hz
Excitation and measurement conditions		
Excitation type	–	Free (sudden release), Sinusoidal force
Input forces (rms)	F_{in}	1.6, 3.6, 5.8, 9.8, 11.8, 15.6, 18.6, 22.5, 25.0, 28.8 N
Measured responses	–	Tip displacement, acceleration, contact force

2.2. Free Response

The free response computed from the simulations is presented in Figure 2. The response is given for different values of the initial displacement applied to the free end of the beam to initiate the motion. These values range from the initial value of 4 mm to the largest displacement of 10 mm, increasing in 1 mm steps, depicted as virtual tests 1 to 7 in the figure. The free response is presented in acceleration and displacement amplitudes, as well as the corresponding frequency content (FFT) of the acceleration response. The contact force between the vibro-impact support and the beam is included. It is important to note that for the first value of the 4 mm tip displacement considered, no contact is experienced as this value equals the gap between the impact support and the beam. However, as the initial displacement increases, the tip of the beam impacts the support. The calculated contact force shows the impact timing, with more impacts occurring as the initial displacement increases. This effect can also be observed in the acceleration response, showing the peaks that represent the occurrence of impacts. The frequency contents of the response also show a recurrence of the second and third harmonics corresponding to the second and third natural frequencies of the beam, respectively. As the initial displacement increases, the response of the beam becomes nonlinear and higher harmonics or additional modes can be excited, leading to the increase in contribution corresponding to the frequency peaks at the second and third natural frequencies. This effect suggests that the energy distribution and dissipation is shifted to higher frequencies because of the repeating impacts. For the larger amplitudes, the shape of the resonance peaks showing a spread in frequency suggests strong nonlinearity that could include higher harmonics due to harmonic distortion, especially when the initial displacement exceeds the linear range of the system.

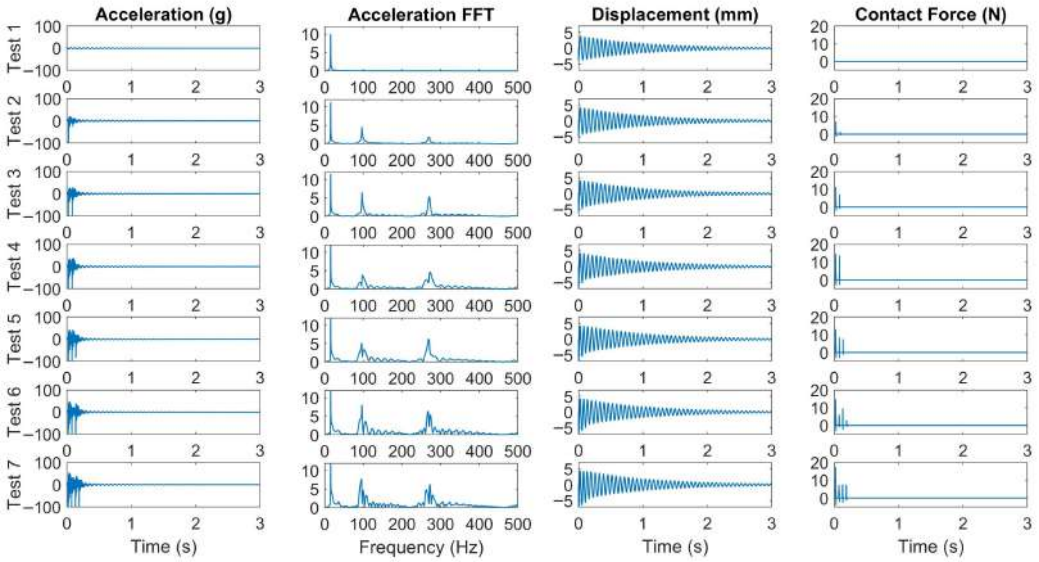

Figure 2. Theoretical free response of the impact damper for different initial displacements.

2.3. Forced Response

On the other hand, Figure 3 shows the forced response given for increasing input force values. This example is calculated for a fixed frequency of 16 Hz close to the first resonant frequency. Tip acceleration in the time and frequency domains, displacement response, and impact force are presented. The peak amplitude input forces considered for virtual tests 1 to 10 are given in Table 1 to match the forces considered in the experimental campaign.

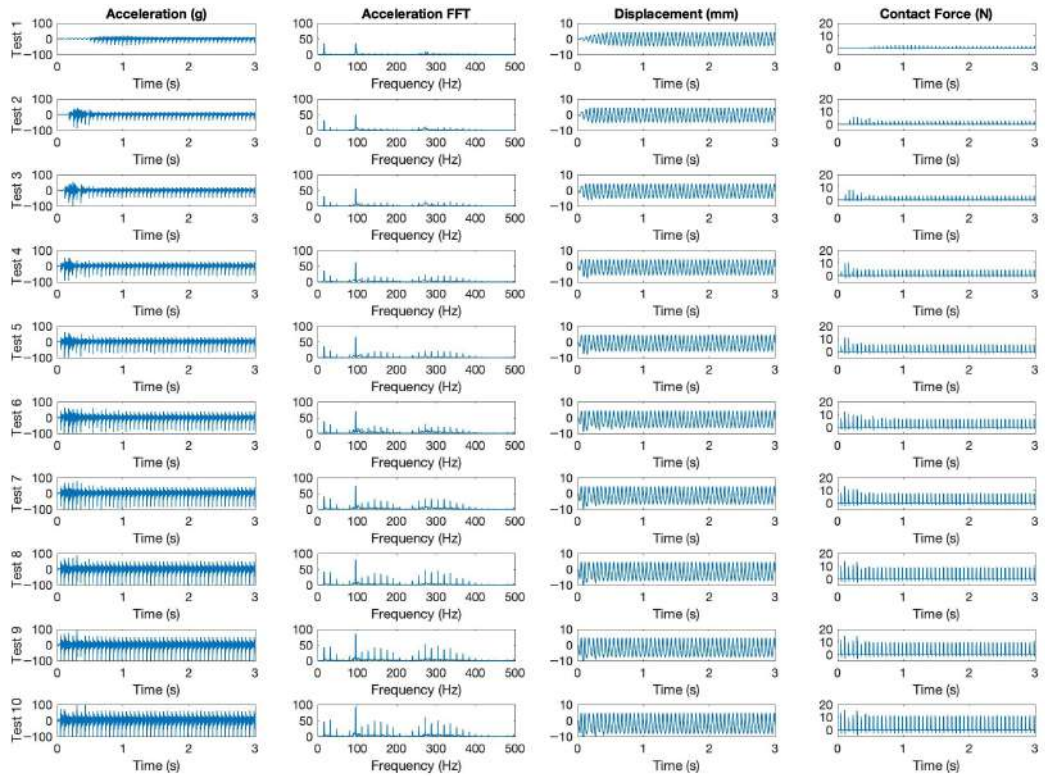

Figure 3. Theoretical forced response of the impact damper for different values of the input force.

The increasing input force leads to stronger impacts, which introduce nonlinear damping effects. However, the frequency content also shows a prominent second harmonic while the third harmonic appears for large values of the input force, with sidebands spread at the

excitation frequency of 16 Hz around the main resonance peaks. As a result, higher input forces excite additional modes, as evidenced by the spectral content. The impact damper is effective in modifying the system dynamics by redistributing energy into different frequency components. The results suggest a transition from a linear regime to a nonlinear impact-dominated regime. The repetitive behaviour of impacts creates a spectrum with additional frequency content. The sidebands that appear around the main harmonics at 16 Hz, 97 Hz, and 270 Hz, spaced by 16 Hz, suggest a modulation effect on the system response. This phenomenon is typically associated with nonlinear interactions as the impact damper introduces nonlinearities due to intermittent contact. As each impact acts as a periodic perturbation, the response of the system is modulated at the excitation frequency, creating sidebands at integer multiples of 16 Hz around the dominant frequencies. This energy redistribution can amplify or suppress certain frequencies depending on the impact conditions.

Discrete values of the forcing frequency are also considered. The frequency response is presented in Figure 4 comparing the linear system with the impacting response for different values of the input force.

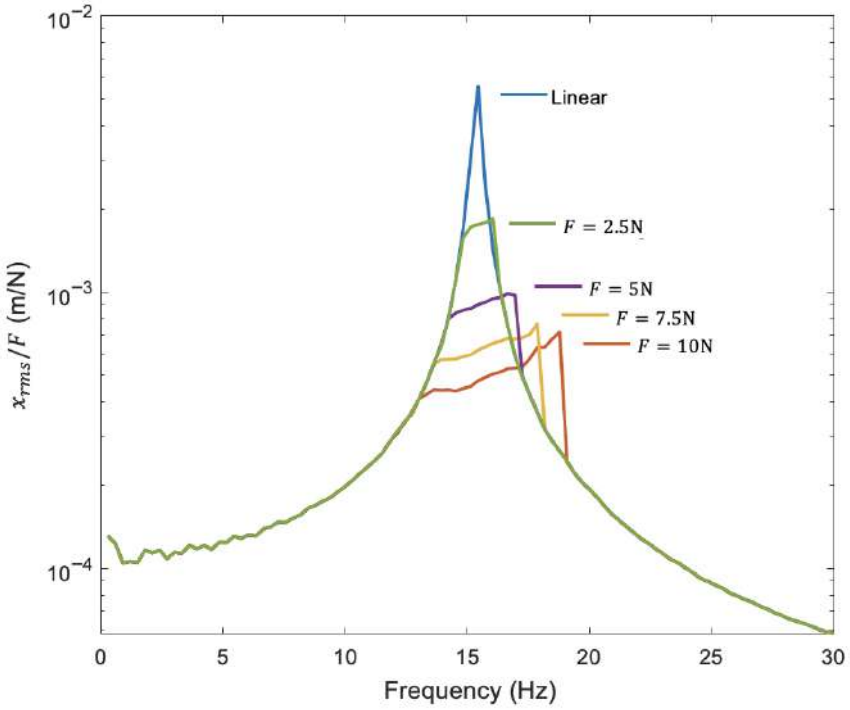

Figure 4. Numerical response (receptance) of the vibro-impacting beam for different values of the input force given with reference to the displacement rms.

3. Experimental Characterization

3.1. The Test Rig

The proposed experimental device comprises an aluminum cantilever beam of length 0.4 m, width 38 mm and thickness of 3 mm, supported by an aluminum frame. The vibro-impact support is a silicone rubber cylinder of 30 mm diameter and 12 mm height, its mass is 10 gr, and the equivalent stiffness measured during uniaxial compression test is 22 KN/m. The rubber support is attached to the fixed frame. There is a 4 mm gap between the impact damper and the beam. An accelerometer is placed on the tip of the beam to record its acceleration. By means of a sudden release of the beam from an initial prescribed displacement, the mass impacts the damper in free vibration. The value of the initial displacement was varied from 4 to 10 mm in 1 mm intervals to match the analytical

simulations. For each case, ten single measurements were recorded and then averaged. Data acquisition was set up to a frequency span of 500 Hz and 1600 lines of resolution resulting in data length of 3.2 s. Real time processing was used during the acquisition to obtain the FFT analysis. Schematics and a photo of the experimental setup are presented in Figure 5.

For the case of forced vibration response, a shaker is attached through a stinger and a mechanical impedance sensor at 70 mm from the fixed support. hlrReal time processing was used in the signal analyzer, considering 30 averages, a frequency span of 800 Hz resulting in data segments of 2 s each, 50 % overlap and Hanning window. The input forces are given in Table 1. The setup and photograph of this configuration are shown in Figure 6.

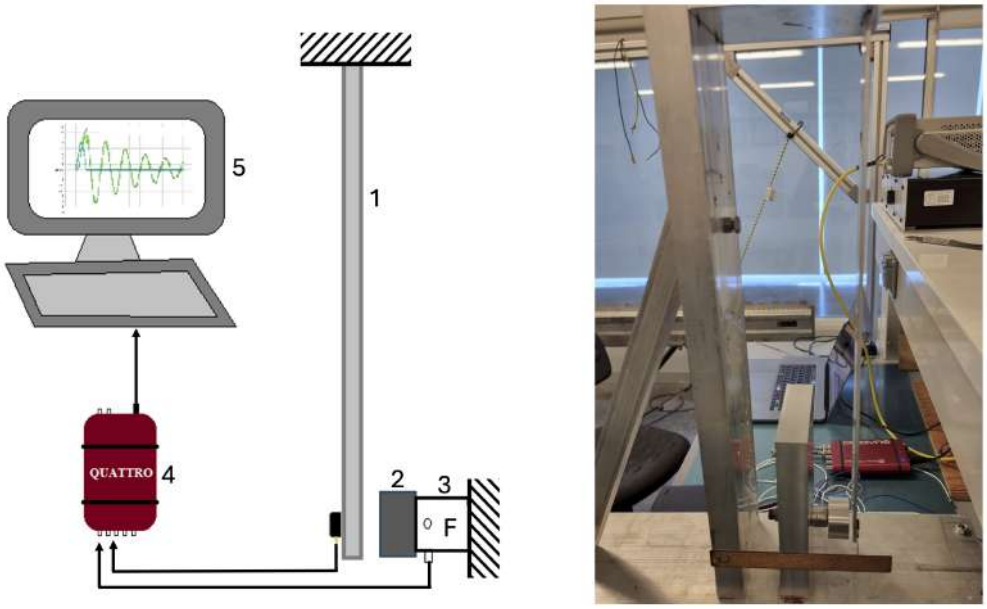

Figure 5. Schematics and picture of the experimental rig for free vibration. (1) Cantilever beam, (2) soft impact damper, (3) force sensor (4) dynamic signal analyzer, (5) PC based data acquisition system.

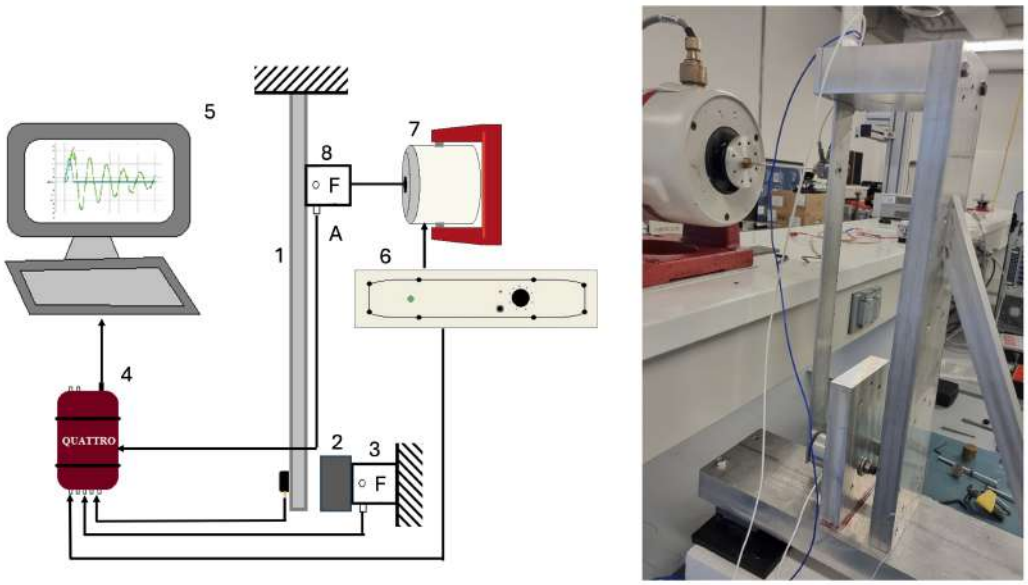

Figure 6. Schematics and picture of the experimental rig for forced vibration. (1) Cantilever beam, (2) soft impact damper, (3) accelerometer (4) DC electromagnet, (5) DC power supply, (6, 7) PC based data acquisition system, (8) mechanical impedance sensor.

3.2. Free Vibration Results

Figure 7 shows the experimental free response results for the different values of the initial displacement considered. The observed trend is similar to the theoretical analysis presented in Figure 2. Impacts are not recorded for the first test with an imposed initial displacement of 4 mm, but as the initial displacement is larger, more impacts appear. As before, the occurrence of the second and third natural frequencies in the frequency analysis suggests nonlinear effects and the spreading of the response at higher frequencies, thus dissipating energy into higher modes. The spread of the resonance peaks is also observed for the largest responses, suggesting other nonlinear effects due to the large displacements are taking place.

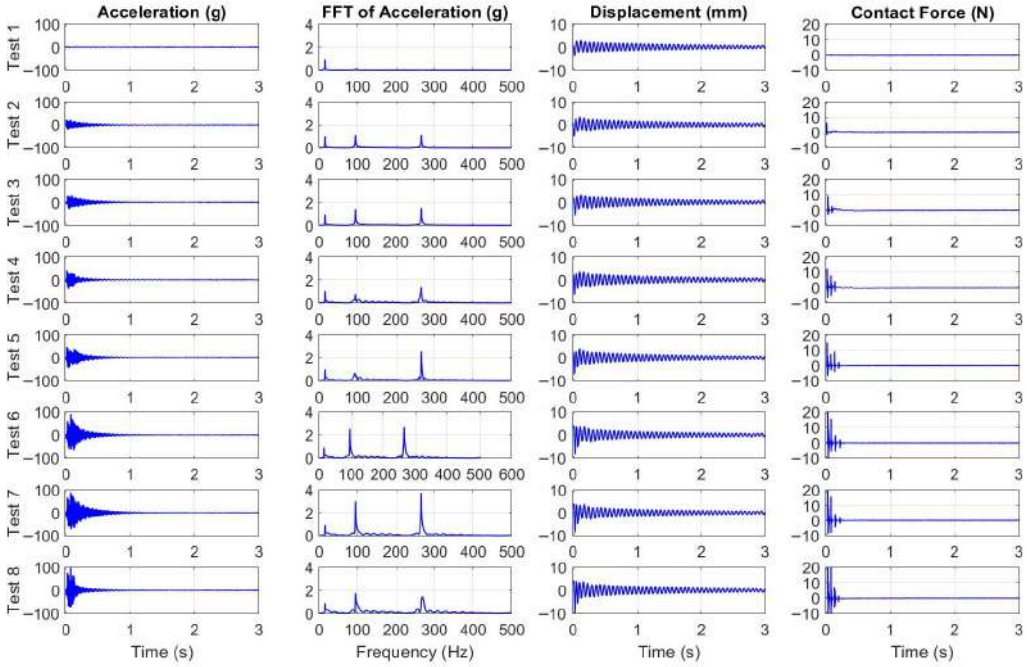

Figure 7. Experimental free response of the impact damper for different initial displacements.

3.3. Forced Vibration Results

When forced vibration is considered, the experimental response is presented in Figure 8. The different cases for increasing values of the external force at a fixed frequency of 16 Hz are shown, to match the theoretical analysis. The same values of the input force considered in the simulations were used in the experiments, as given in Table 1. The predicted effects in the theoretical analysis are validated in this experiment, where the nonlinear effects are evident. It appears that the dominant peaks match the fundamental excitation frequency of 16 Hz as well as the second and third natural frequencies of the beam. Higher input forces lead to more pronounced frequency components, indicating nonlinear effects such as impacts that excite higher modes. The previously observed sidebands are also present in the experimental results. As a result, the intermittent impacting creates a spectrum with additional frequency content, demonstrating the capability in modifying the system dynamics by redistributing energy into different frequency components which can result in improved energy dissipation.

The experimental response has been obtained as the ratio between several discrete forcing frequencies and different input amplitudes, and it is presented in Figure 9. This plot was obtained by measuring the steady state tip response when the external force was applied at a fixed frequency. The acceleration response was processed to estimate the displacement response. The output/input root mean square (rms) amplitude ratio was

then estimated. The tests were performed starting at a frequency of 10 Hz up to a frequency of 25 Hz in 1 Hz steps. The input force values of the rms considered were 2 N (resulting in a linear system since no impact was observed) and then 3.7 N, 6.7 N, 10 N, 14.7 N and 18 N for the vibro-impact response.

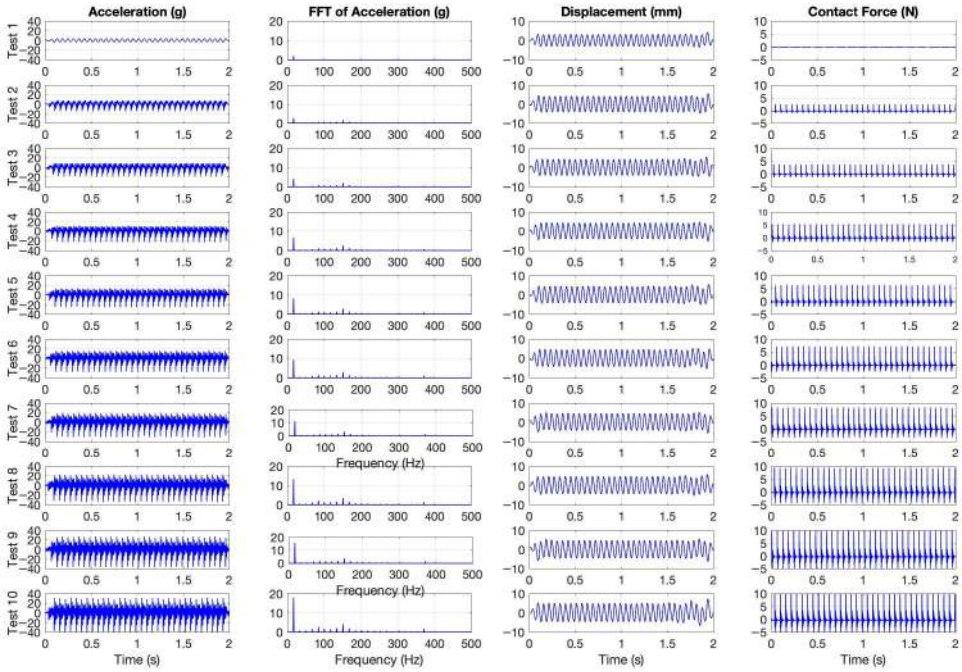

Figure 8. Experimental forced response of the impact damper for different values of the excitation force.

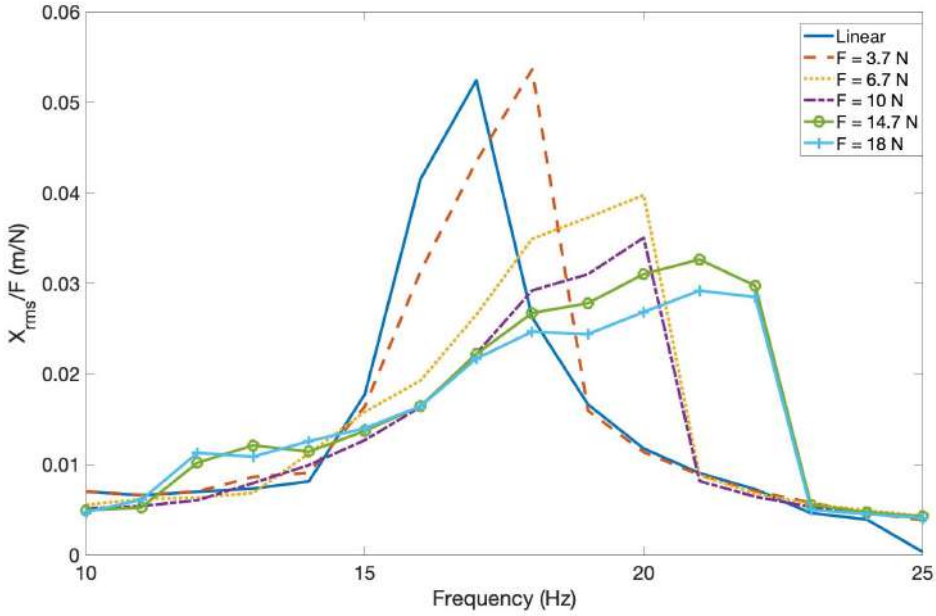

Figure 9. Experimental response (receptance) of the vibro-impacting beam for different values of the input force given with reference to the displacement rms.

4. Discussion on Theoretical and Experimental Results

Consistent agreement is observed between theoretical simulations and experimental measurements for free and forced responses (Figures 10 and 11). These figures present comparisons between the theoretical model and experimental validation for specific scenarios, i.e., an initial displacement of 100 mm for free vibration, and an input force of 12 N at

16 Hz. These experiments validate the main trends predicted by the model, confirming the excitation of higher-order modes and the broadening of the resonance region as a function of increasing amplitude or input force. These effects arise from the nonlinear nature of the vibro-impact interaction, where repeated contacts introduce strong coupling between the fundamental and higher modes of vibration.

These observed phenomena, namely the resonance broadening and the activation of higher-order modes, are direct manifestations of the fundamental nonlinear energy transfer mechanisms enabled by the vibro-impact interaction. Such mechanisms are a well-established feature of nonlinear vibration absorbers, such as Nonlinear Energy Sinks (NESs), where they enable passive and broadband energy dissipation [9,44]. As analyzed by [45,46], the impulsive, non-smooth nature of impacts induces two synergistic effects: inter-modal energy scattering and targeted energy transfer. Inter-modal energy scattering refers to the broadband redistribution of vibrational energy from the directly excited fundamental mode into higher structural eigenmodes, facilitated by the frequency mixing inherent to nonlinear impacts. Concurrently, targeted energy transfer describes the irreversible channeling of a portion of this scattered energy into the localized modes of the vibro-impact attachment itself, where it is subsequently dissipated. This dual mechanism explains the effective vibration suppression over an extended frequency range, as the system's response is no longer governed by a single, sharp resonance but is instead averaged and dissipated across multiple modes [47]. Although this work focuses on a compliant vibro-impact support, the core physical principles of nonlinear energy scattering and transfer are analogous.

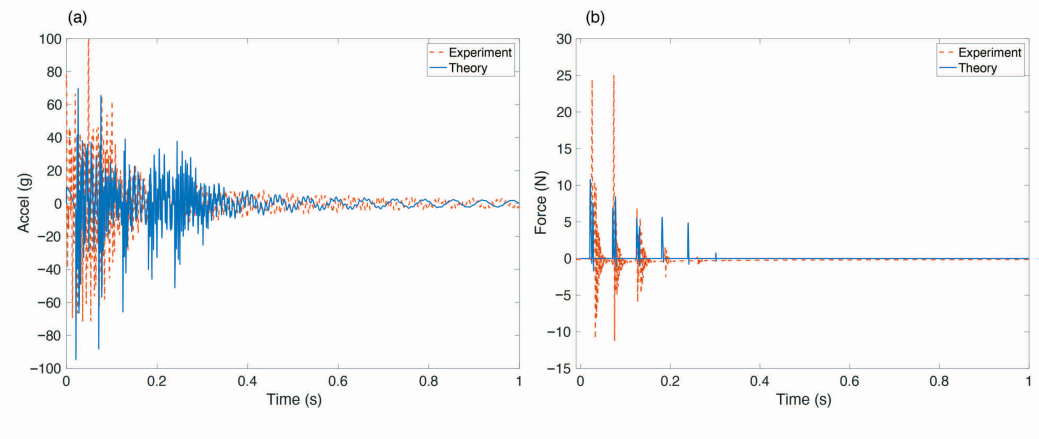

Figure 10. Comparison between simulation and experimental tests of the free response for an initial displacement of 10 mm. (**a**) Tip acceleration. (**b**) Contact force.

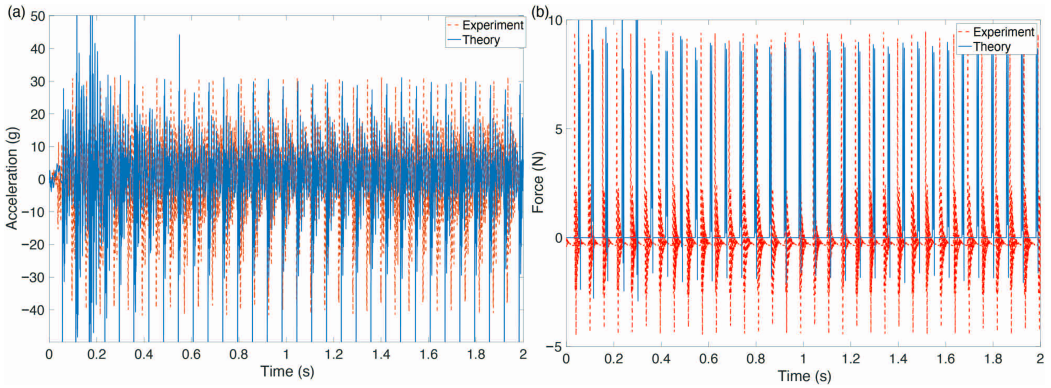

Figure 11. Comparison between simulation and experimental of the forced response for an input force of 12 N. (**a**) Tip acceleration. (**b**) Contact force.

In the current configuration, impacts with the viscoelastic support contribute to enhance energy dissipation by shifting vibrational energy from the dominant (first) mode to higher-order modes, where damping is more effective. This impact-induced mode coupling mechanism has been widely recognized as a characteristic of nonlinear damping and is consistent with the numerical predictions of this work. The experimental frequency spectra confirm the presence of sidebands and higher harmonics, indicating modulation effects similar to those associated with non-resonant energy transfer in theoretical VIC models.

Figure 4 illustrates the simulated frequency response of the system to increasing excitation amplitudes. At low forcing levels, the system behaves linearly, showing a single sharp resonance peak near the first natural frequency. As the input force increases and the beam begins to contact the soft support, impacts introduce additional stiffness and damping. The resonance peak becomes broader and slightly shifts toward higher frequencies, indicating amplitude-dependent dynamic stiffness. At higher excitation levels, the curve flattens, which is characteristic of nonlinear systems with intermittent contact. These distortions in the receptance curve reflect the redistribution of vibrational energy from the fundamental mode toward higher harmonics, effectively increasing dissipation. Furthermore, the experimental results presented in Figure 9 show a very similar trend. For the smallest input force (approximately 2 N), the system remains in the linear regime and no impacts occur, resulting in a sharp resonance near 16 Hz. As the input force increases beyond the impact threshold, the resonance peak broadens and its amplitude decreases, matching the nonlinear damping behavior predicted numerically. The progressive flattening and widening of the experimental frequency response at higher force levels confirm that the system transitions from a linear resonant regime to a nonlinear impact-dominated regime. The similarity in the shape and evolution of the numerical and experimental receptance curves demonstrates that the model accurately captures the essential nonlinear dynamics of the vibro-impact damper.

The observed spectral broadening and emergence of higher-frequency components are consistent with the theoretical mechanisms of nonlinear energy interactions described by Vyas [3]. In the later reference, vibro-impacting cantilevers (VICs) were shown to exhibit both resonant and non-resonant energy transfers between modes, producing amplitude modulation, subharmonic resonances, and quasi-periodic responses through Harmonic Resonance Energy Stimulation (HRES). Although the present study does not explicitly resolve the secondary jump or quasi-periodic dynamics predicted by Vyas, the redistribution of spectral energy to higher frequencies observed in both free and forced experiments provides experimental evidence of similar nonlinear energy pathways. These higher frequency contents suggest that energy dissipation occurs through impact-induced mode coupling, validating the predictions from numerical simulations.

Table 2 shows a summary of the theoretical and experimental findings as presented in Figures 10 and 11. Although some discrepancies between theoretical and experimental results are found, in particular for the case of free vibration peak contact force, those can be attributed to simplifications in the model, such as the assumption of idealized contact and constant damping parameters. In practice, factors such as the viscoelastic nonlinearity of the silicone interface, variations in the coefficient of restitution, and imperfections in the boundary condition can alter the dynamics of the contact. Nevertheless, the close correlation between the simulation and the experimental results demonstrates that the proposed impact damper model effectively captures the dominant nonlinear mechanisms governing energy redistribution and dissipation.

Table 2. Quantitative comparison between theoretical predictions and experimental measurements for selected vibration cases.

Case/Input Condition	Parameter	Theory	Experiment	Deviation (%)
Linear Regime ($F_{in} \approx 2$ N)	1st Natural Freq.	15.4 Hz	16.0 Hz	3.9%
Nonlinear Forced ($F_{in} = 12$ N, 16 Hz)	Peak Tip Accel.	52 g	41 g	26.8%
	Peak Contact Force	10.0 N	9.4 N	6.3%
Nonlinear Free (Init. Disp. = 10 mm)	Peak Tip Accel.	107 g	95 g	12.6%
	Peak Contact Force	10 N	25 N	60%

From a machine design perspective, the transition of the cantilever system into a nonlinear impact-dominated regime under high-force conditions provides a versatile mechanism for broadband damping. The selection of a viscoelastic silicone rubber interface is particularly advantageous for industrial machinery because of its material durability and the capacity for controlled stiffness variation. These experimental results suggest that such isolators could be effectively scaled and integrated into larger mechanical frameworks, such as automotive suspension systems or structural dampers, i.e., end stop impacts and buffers. Furthermore, the occurrence of predictable higher-frequency components and sidebands could serve as a diagnostic feature, allowing passive monitoring of machine health through impact-induced modal signatures. Overall, this work complements the purely theoretical studies of vibro-impacting beams by providing experimental validation of nonlinear impact dynamics and mode coupling. The findings emphasize that properly tuned impact dampers can take advantage of these nonlinear mechanisms to enhance vibration suppression through dynamic energy redistribution, bridging the gap between theoretical predictions and practical implementation in machines and structural systems. Despite these advantages, practical implementation requires careful consideration of physical constraints. The device's effectiveness relies on maintaining a precise gap distance, which may be challenging in space-constrained environments where clearance is limited. Furthermore, while the viscoelastic interface significantly reduces peak forces compared to hard impacts, long-term durability regarding material fatigue and wear from repetitive high-frequency impacts remains a critical factor for service life. However, even with these constraints, the proposed soft-impact configuration is highly promising for scalable applications, particularly as end-stop buffers in automotive suspension systems or robotic actuators. In these scenarios, the damper can effectively function as a secondary safety mechanism, preventing structural damage from limit-cycle oscillations while providing supplementary broadband damping.

Future work will extend this research in two specific technical directions. First, the investigation could consider multi-degree-of-freedom (MDOF) systems by coupling the impact damper to a primary oscillator. This will allow for the analysis of Targeted Energy Transfer (TET) efficiency and the suppression of specific structural modes through energy pumping. Second, to account for the limitations of passive tuning, semi-active control strategies can be implemented by replacing the passive silicone interface with Magnetorheological Elastomers (MREs). This methodology will enable real-time modulation of the contact stiffness via an external magnetic field. Subsequent research will focus on investigating control strategies such as on-off stiffness switching or phase-based control to maximize energy dissipation across varying excitation frequencies and transient load conditions.

5. Conclusions

This work presented a combined theoretical and experimental study of a vibro-impacting cantilever beam equipped with a soft impact interface, aimed at characterizing its nonlinear dynamic response and damping performance. From an engineering design perspective, this study establishes three key guidelines for implementing soft vibro-impact dampers.

First, effective broadband suppression relies on tuning the system to operate specifically in the nonlinear impact-dominated regime. The experimental results demonstrate that pushing the system beyond the linear threshold where resonance peaks flatten and widen is necessary to trigger the energy redistribution mechanisms required for robust damping.

Second, the selection of a viscoelastic interface offers distinct advantages over traditional hard stops. Beyond simple momentum exchange, the soft interface introduces material damping and nonlinear stiffness that facilitate inter-modal energy scattering to higher harmonics, reducing vibration amplitude while protecting the host structure from high-force transient shocks.

Third, the close correlation between the numerical model and experimental trials confirms that the impact gap and contact stiffness can be treated as precise tuning variables. This validates the proposed model as a reliable design tool for predicting the onset of nonlinear damping and optimizing the damper configuration before physical prototyping.

In summary, the integration of theoretical modeling and experimental validation has demonstrated that soft-contact vibro-impact systems can achieve enhanced damping through amplitude-dependent nonlinear dynamics. Future work will focus on extending the approach to multi-degree-of-freedom configurations and exploring adaptive or semi-active implementations to broaden the operational frequency range and improve controllability.

Author Contributions: Conceptualization, D.F.L.-R. and E.R.; methodology, D.F.L.-R. and E.R.; software, D.F.L.-R. and E.R.; validation, D.F.L.-R. and P.E.T.G.; formal analysis, D.F.L.-R.; investigation, D.F.L.-R. and P.E.T.G.; resources, D.F.L.-R. and P.E.T.G.; data curation, D.F.L.-R. and P.E.T.G.; writing—original draft preparation, D.F.L.-R. and E.R.; writing—review and editing, D.F.L.-R., E.R. and P.E.T.G. All authors have read and agreed to the published version of the manuscript.

Funding: This research received no external funding.

Data Availability Statement: The raw data supporting the conclusions of this article will be made available by the authors on request.

Conflicts of Interest: The authors declare no conflicts of interest.

References

1. Ledezma-Ramírez, D.F.; Tapia-González, P.E.; Ferguson, N.; Brennan, M.; Tang, B. Recent advances in shock vibration isolation: An overview and future possibilities. *Appl. Mech. Rev.* **2019**, *71*, 060802. [CrossRef]
2. Blazejczyk-Okolewska, B. Analysis of an impact damper of vibrations. *Chaos Solitons Fractals* **2001**, *12*, 1983–1988. [CrossRef]
3. Vyas, V. On the nonlinear energy interactions in vibro-impacting cantilever. *J. Vib. Control* **2025**, *31*, 1829–1839. [CrossRef]
4. Lu, Z.; Wang, Z.; Masri, S.F.; Lu, X. Particle impact dampers: Past, present, and future. *Struct. Control Health Monit.* **2018**, *25*, e2058. [CrossRef]
5. Akbar, M.A.; Wong, W.O.; Rustighi, E. Design optimization of a single-mass impact damper. *J. Sound Vib.* **2024**, *570*, 118019. [CrossRef]
6. Akbar, M.A.; Qin, Q. Experimental investigation of particle impact dampers: Vibration reduction and noise levels with varied particle numbers. In *Proceedings of the Structures*; Elsevier: Amsterdam, The Netherlands, 2024; Volume 69, p. 107407.
7. Akbar, M.A.; Wong, W.; Rustighi, E. A study of soft and hard impact effects in single-particle impact dampers. *J. Vib. Control* **2025**, *31*, 3357–3370. [CrossRef]
8. Son, L.; Kawachi, M.; Matsuhisa, H.; Utsuno, H. Reducing floor impact vibration and sound using a momentum exchange impact damper. *J. Syst. Des. Dyn.* **2007**, *1*, 14–26. [CrossRef]

9. Karayannis, I.; Vakakis, A.; Georgiades, F. Vibro-impact attachments as shock absorbers. *Proc. Inst. Mech. Eng. Part C J. Mech. Eng. Sci.* **2008**, *222*, 1899–1908. [CrossRef]
10. Son, L.; Kawachi, M.; Matsuhisa, H.; Utsuno, H. Energy transfer mechanism in a three-body momentum exchange impact damper. *J. Sound Vib.* **2008**, *2*, 425–438.
11. Weidemann, T.; Bergman, L.A.; Vakakis, A.F.; Krack, M. Energy transfer and localization in a forced cyclic chain of oscillators with vibro-impact nonlinear energy sinks. *Nonlinear Dyn.* **2025**, *113*, 14319–14360. [CrossRef]
12. Li, X.; Mojahed, A.; Wang, C.; Chen, L.Q.; Bergman, L.A.; Vakakis, A.F. Irreversible energy transfers in systems with particle impact dampers. *Nonlinear Dyn.* **2024**, *112*, 35–58. [CrossRef]
13. Qiu, D.; Seguy, S.; Paredes, M. Design criteria for optimally tuned vibro-impact nonlinear energy sink. *J. Sound Vib.* **2019**, *442*, 497–513. [CrossRef]
14. Zhang, J.; Lu, Z.; Zhou, M.; Huang, Z.; Masri, S.F. Experimental and numerical study on the dynamic behavior of a semi-active impact damper. *Smart Struct. Syst. Int. J.* **2023**, *31*, 455–467.
15. Son, L.; Hara, S.; Matsuhisa, H.; Utsuno, H.; Yamada, K. Proposal of active momentum exchange impact damper and its application to floor shock vibration control. In Proceedings of the 2008 SICE Annual Conference, Chofu, Japan, 20–22 August 2008; pp. 806–811. [CrossRef]
16. Son, L.; Hara, S.; Yamada, K.; Matsuhisa, H. Experiment of shock vibration control using active momentum exchange impact damper. *J. Vib. Control* **2010**, *16*, 49–64. [CrossRef]
17. Son, L.; Kawachi, M.; Matsuhisa, H.; Utsuno, H. Development of an active momentum exchange impact damper for floor shock vibration control. *J. Sound Vib.* **2008**, *2*, 930–945.
18. Kushida, Y.; Hara, S.; Otsuki, M.; Yamada, Y.; Hashimoto, T.; Kubota, T. Robust landing gear system based on a hybrid momentum exchange impact damper. *J. Guid. Control. Dyn.* **2013**, *36*, 776–789. [CrossRef]
19. Saed, M.O.; Elmadih, W.; Terentjev, A.; Chronopoulos, D.; Williamson, D.; Terentjev, E.M. Impact damping and vibration attenuation in nematic liquid crystal elastomers. *Nat. Commun.* **2021**, *12*, 6676. [CrossRef] [PubMed]
20. Guo, H.; Terentjev, A.; Saed, M.O.; Terentjev, E.M. Momentum transfer on impact damping by liquid crystalline elastomers. *Sci. Rep.* **2023**, *13*, 10035. [CrossRef]
21. Ledezma-Ramírez, D.F.; Rustighi, E.; Tapia-González, P.E. Design of a Variable Stiffness Impact Damper Using Magnetorheological Elastomers. In *Proceedings of the Sensors & Instrumentation and Aircraft/Aerospace Testing Techniques*; Walber, C., Stefanski, M., Seidlitz, S., Eds.; Springer: Cham, Switzerland, 2024; Volume 8, pp. 87–90.
22. Rahmat, M.S.; Hudha, K.; Abd Kadir, Z.; Nuri, N.R.M.; Amer, N.H.; Abdullah, S. Modelling and control of a Magneto-Rheological elastomer for impact reduction. *J. Mech. Eng. Sci.* **2019**, *13*, 5259–5277. [CrossRef]
23. Rahmat, M.S.; Hudha, K.; Abd Kadir, Z.; Amer, N.H.; Mohamad Nor, N.; Choi, S.B. A hybrid skyhook active force control for impact mitigation using magneto-rheological elastomer isolator. *Smart Mater. Struct.* **2021**, *30*, 025043. [CrossRef]
24. Son, L.; Matsuhisa, H.; Utsuno, H. A Novel Boat Shock Vibration Control using Momentum Exchange Principle with Pre-Straining Spring Mechanism. *Int. J. Automot. Mech. Eng.* **2020**, *17*, 7858–7867. [CrossRef]
25. Badri, Y.; Sassi, S.; Hussein, M.; Renno, J. Experimental and numerical investigation of damping in a hybrid automotive damper combining viscous and multiple-impact mechanisms. *J. Vib. Control* **2022**, *28*, 3676–3687.
26. Ganci, C.; Kuether, R.; Hurlebaus, S. Validation of a Tapered Impact Damper for Traffic Signal Structure Vibrations Using the Method of Harmonic Balance. *Exp. Tech.* **2024**, *49*, 327–340. [CrossRef]
27. Darmawan, D.; Lovelyson, L.; Rusli, M.; Kurnia, R. Simulation and Experimental of PSMEID with Preview for Controlling Shock Vibration on UAV's Landing Gear. *TEM J.* **2025**, *14*, 447–462. [CrossRef]
28. Li, Z.; Du, Y. Interval of restitution coefficient for chattering in impact damper. *J. Low Freq. Noise Vib. Act. Control* **2022**, *41*, 432–450. [CrossRef]
29. Gong, C.; Fang, X.; Cheng, L. Multi-state dynamics and model similarity of a vibro-impact nonlinear system. *Int. J.-Non-Linear Mech.* **2024**, *163*, 104765. [CrossRef]
30. Lizunov, P.; Pogorelova, O.; Postnikova, T. Influence of stiffness parameters on vibro-impact damper dynamics. *Strength Mater. Theory Struct.* **2023**, *110*, 21–35. [CrossRef]
31. Lizunov, P.; Pogorelova, O.; Postnikova, T.; Gerashchenko, O. Influence of mass on the efficiency and dynamics of single-sided and double-sided vibro-impact nonlinear energy sinks. *Strength Mater. Theory Struct.* **2024**, *113*, 3–17.
32. Lizunov, P.; Pogorelova, O.; Postnikova, T. Comparison of the performance and dynamics of the asymmetric single-sided and symmetric double-sided vibro-impact nonlinear energy sinks with optimized designs. *Int. J. Mech. Syst. Dyn.* **2024**, *4*, 303–316. [CrossRef]
33. Davies, H. Random vibration of a beam impacting stops. *J. Sound Vib.* **1980**, *68*, 479–487. [CrossRef]
34. Bishop, S.; Thompson, M.; Foale, S. Prediction of period-1 impacts in a driven beam. *Proc. R. Soc. London. Ser. A Math. Phys. Eng. Sci.* **1996**, *452*, 2579–2592.

35. Wagg, D.; Karpodinis, G.; Bishop, S. An experimental study of the impulse response of a vibro-impacting cantilever beam. *J. Sound Vib.* **1999**, *228*, 243–264. [CrossRef]
36. Lin, W.; Qiao, N.; Yuying, H. Bifurcations and chaos in a forced cantilever system with impacts. *J. Sound Vib.* **2006**, *296*, 1068–1078. [CrossRef]
37. Ervin, E.K.; Wickert, J. Repetitive impact response of a beam structure subjected to harmonic base excitation. *J. Sound Vib.* **2007**, *307*, 2–19. [CrossRef]
38. Luo, G.; Xie, J.; Zhu, X.; Zhang, J. Periodic motions and bifurcations of a vibro-impact system. *Chaos Solitons Fractals* **2008**, *36*, 1340–1347. [CrossRef]
39. Gandhi, P.; Vyas, V. On the dynamics of tapered vibro-impacting cantilever with tip mass. *J. Mech. Sci. Technol.* **2017**, *31*, 63–73. [CrossRef]
40. Ibrahim, R. Recent advances in nonlinear passive vibration isolators. *J. Sound Vib.* **2008**, *314*, 371–452. [CrossRef]
41. Ding, H.; Chen, L.Q. Designs, analysis, and applications of nonlinear energy sinks. *Nonlinear Dyn.* **2020**, *100*, 3061–3107. [CrossRef]
42. Su, X.; Kang, H.; Guo, T. Modelling and energy transfer in the coupled nonlinear response of a 1: 1 internally resonant cable system with a tuned mass damper. *Mech. Syst. Signal Process.* **2022**, *162*, 108058. [CrossRef]
43. Zhang, Y.; Li, J.; Wu, Q.; Amabili, M.; Misseroni, D.; Jiang, H. Viscoelastic structural damping enables broadband low-frequency sound absorption. *Proc. Natl. Acad. Sci. USA* **2025**, *122*, e2520808122. [CrossRef]
44. Nucera, F.; Vakakis, A.F.; McFarland, D.M.; Bergman, L.; Kerschen, G. Targeted energy transfers in vibro-impact oscillators for seismic mitigation. *Nonlinear Dyn.* **2007**, *50*, 651–677. [CrossRef]
45. Zhang, B.; Zhang, Z.; Jiang, J.; Zhang, Y.; Li, B.; Li, H.; Xian, H. Advantages of vibro-impact nonlinear energy sinks for vibration suppression of continuous systems: Coexistence of inter-modal energy scattering and targeted energy transfer. *Commun. Nonlinear Sci. Numer. Simul.* **2025**, *151*, 108993. [CrossRef]
46. Shi, B.; Yang, J.; Wiercigroch, M. Vibrational energy transfer in coupled mechanical systems with nonlinear joints. *Int. J. Mech. Sci.* **2023**, *260*, 108612. [CrossRef]
47. Yang, Y.; Liu, C.; Lai, S.K.; Chen, Z.; Chen, L. Frequency-dependent equivalent impedance analysis for optimizing vehicle inertial suspensions. *Nonlinear Dyn.* **2025**, *113*, 9373–9398. [CrossRef]